Effect of SiO$_2$ on the thermal stability and spectroscopic properties of Er^{3+}-doped tellurite glasses*

ZHENG Shi-chao (郑世超)** **and ZHOU Ya-xun** (周亚训)

College of Information Science and Engineering, Ningbo University, Ningbo 315211, China

Er^{3+}-doped tellurite glass (TeO$_2$-ZnO-Na$_2$O) prepared using the conventional melt-quenching method is modified by introducing the SiO$_2$, and its effects on the thermal stability of glass host and the 1.53 μm band spectroscopic properties of Er^{3+} are investigated by measuring the absorption spectra, 1.53 μm band fluorescence spectra, Raman spectra and differential scanning calorimeter (DSC) curves. It is found that for Er^{3+}-doped tellurite glass, besides improving its thermal stability, introducing SiO$_2$ is helpful for the further improvement of the fluorescence full width at half maximum (FWHM) and bandwidth quality factor. The results indicate that the prepared Er^{3+}-doped tellurite glass containing an appropriate amount of SiO$_2$ has good prospect as a candidate of gain medium applied for 1.53 μm broadband amplifier.

With the increasing need for telecom bandwidth, the development of novel optical amplifiers offering wider spectrum and higher gain than current technologies is an urgent research topic. Most current amplifying technologies rely on Er^{3+}-doped fiber amplifier (EDFA) made from silica glass fiber. However, the typical gain bandwidth is only about 35 nm in the 1.53 μm band, which cannot meet the future needs for broadband transmission[1]. Er^{3+}-doped tellurite glass exhibits a large stimulated emission cross-section and a broad fluorescence full width at half maximum (FWHM) at 1.53 μm band[2-4]. In addition, tellurite glass also possesses high linear and nonlinear refractive indices, high rare-earth solubility and high gain coefficient. However, its poor glass thermal stability makes it difficult to be used in practice.

It is well known that SiO$_2$ is a good glass former and adding SiO$_2$ into glass can enhance the thermal stability and improve the resistance for crystallization[5]. However, samples containing TeO$_2$ and SiO$_2$ have been investigated very little so far. In this paper, SiO$_2$ is introduced into the Er^{3+}-doped TeO$_2$-ZnO- Na$_2$O glasses. Especially, the effects of SiO$_2$ on the thermal stability, Judd-Ofelt parameters, FWHM and stimulated emission cross-section of Er^{3+}-doped tellurite glass are analyzed and discussed.

The Er^{3+}-doped tellurite glasses with (75-x)TeO$_2$-15ZnO-9.5Na$_2$O-xSiO$_2$-0.5Er$_2$O$_3$ (x=0, 3%, 6%, 9% in mole ratio) were prepared in alumina crucibles at 1000-1100 °C for about 30 min. The obtained glass melts were annealed at about 330 °C for 120 min, and next were cut and well polished for optical measurements. The prepared samples were denoted as TZNS0-3 for short, in which component Na$_2$O was introduced in Na$_2$CO$_3$ form.

The absorption spectra were measured with a Lamda 950 UV/VIS/NIR spectrophotometer in the wavelength range of 400-1700 nm. The fluorescence spectra were measured with a Jobin Yvon Triax550 upon excitation of a 975 nm laser diode (LD). The Raman spectra were measured by a Renishaw Micro-Raman instrument and the thermal stability of glass sample was determined using a differential scanning calorimeter (DSC) of TA Instrument Q2000 at a heating rate of 10 K/min.

Fig.1 displays the measured Raman spectra of TZNS0 and TZNS1 glass samples with and without SiO$_2$. The Raman scattering band centered around 420 cm^{-1} is assigned to the stretching vibrations of Te-O-Te or O-Te-O linkages between two [TeO$_4$] four-coordinate atoms, and the bands centered around 660 cm^{-1} and 750 cm^{-1} originate from the stretching vibrations of Te-O bond in the continuous networks composed of [TeO$_4$] trigonal bipyramid and [TeO$_{3+\delta}$] trigonal pyramid structural units, respectively. A new Raman scattering peak centered around 1370 cm^{-1} is observed in the SiO$_2$ contained glass sample, which is attributed to the characteristic stretching vibration modes of Si-O or Si=O bonds[6].
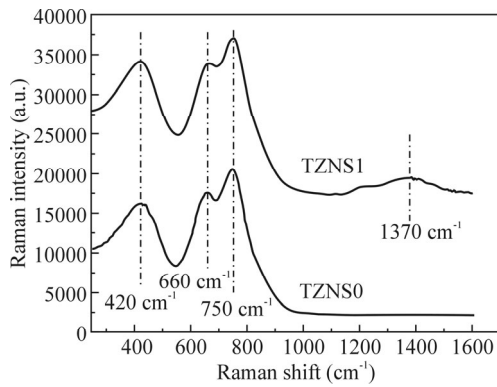
Fig.1 Raman spectra of TZNS0 and TZNS1 glass samples

Fig.2 displays the measured DSC curves of TZNS0-3 glass samples, and the obtained three characteristic temperatures, i.e., glass transition temperature (T_g), crystallization onset temperature (T_x) and the difference ($\Delta T = T_x - T_g$) between them, are recorded in Tab.1.

In general, more than 100 °C for ΔT can satisfy the requirement of conventional fiber drawing process. It can be seen that on the whole, the values of T_g and ΔT for the prepared TZNS1-3 glass samples increase with the substitution of SiO_2 for TeO_2 component. Especially, no obvious crystallization onset peak is found in the glass sample TZNS3. The results indicate that the current investigated TZNS1-3 glasses are more desirable for fiber drawing in view of the thermal stability.
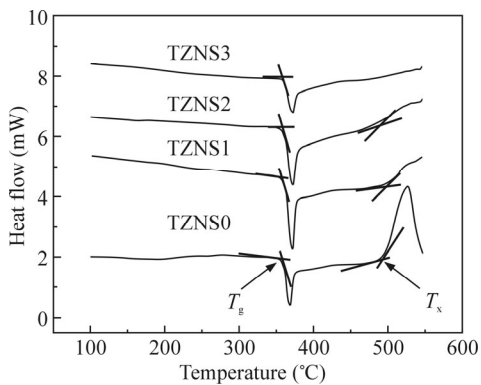
Fig.2 DSC curves of TZNS0-3 glass samples

Fig.3 reveals the measured absorption spectra of the prepared TZNS0-3 glass samples in the wavelength range of 400-1700 nm. All the inhomogeneously broadened absorption bands are attributed to 4f-4f transition of Er^{3+} from the $^4I_{15/2}$ ground state to the different excited states, and their baycenters are found to be almost identical except for some differences in the band intensities. It suggests that the introduction of SiO_2 has no obvious effect on the position of the lowest Stark sub-levels of Er^{3+} manifolds.

The Judd-Ofelt theory[7,8] is a useful tool for analyzing

the spectroscopic properties of rare-earth doped glass or crystal, and is often used to evaluate the spectroscopic parameters, such as the three intensity parameters Ω_t (t=2, 4, 6). The parameters can be acquired from the measured absorption spectrum and the refractive index of glass host by a least-square fitting approach according to the procedure provided in Ref.[9]. The obtained three intensity parameters of the prepared glass samples together with the other glasses are listed in Tab.2.

Tab.1 Glass transition temperature (T_g), crystallization temperature (T_x), and the difference ΔT between them for prepared TZNS0-3 glasses

Sample	T_g (°C)	T_x (°C)	ΔT (°C)
TZNS0	357	470	113
TZNS1	357	498	141
TZNS2	358	491	133
TZNS3	359	-	∞

According to the Tanabe studies[10], the fluorescence emission, produced when Er^{3+} transits from the various excited states to the ground state $^4I_{15/2}$, mainly comes from the contributions of electric-dipole transition. In order to achieve the broad and flat fluorescence emission spectrum, increasing the spectral line strength of electric-dipole transition is an effective way. Here, the spectral line strength of electric-dipole transition can be obtained based on the following linear combination of three intensity parameters[11]

$$S_{ed}[^4I_{13/2} \rightarrow {}^4I_{15/2}]=0.0188\Omega_2 +0.1176\Omega_4+1.4617\Omega_6. \quad (1)$$

From the above equation, it is easily concluded that the spectral line strength S_{ed} mainly depends on the parameter Ω_6, as it has a largest weighted coefficient of 1.4617. Apparently, increasing the parameter Ω_6 can effectively improve the value of S_{ed}. The calculated intensity parameter Ω_6 in this paper has a larger value compared with other glasses, such as silicate, aluminate and germanate[12], indicating that Er^{3+} ions in our prepared tellurite glass are more possible to realize broad emission.
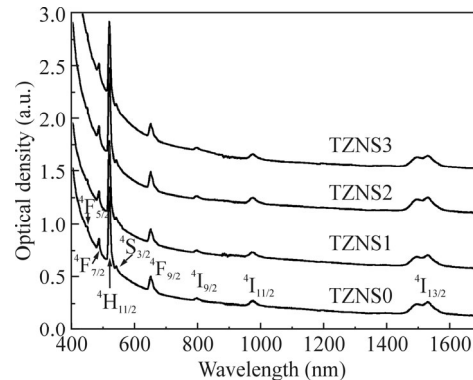

Fig.3 Absorption spectra of TZNS0-3 glass samples

Tab.2 The compositional dependence of Ω_t (t=2, 4, 6) of Er^{3+} in TZNS0—3 samples

Composition	Ω_2 (10^{-20} cm)	Ω_4 (10^{-20} cm)	Ω_6 (10^{-20} cm)
TZNS0	5.39	1.41	0.93
TZNS1	5.82	1.66	0.94
TZNS2	5.87	1.71	0.91
TZNS3	5.75	1.54	1.00
Silicate[13]	4.23	1.04	0.61
Aluminate[13]	5.60	1.60	0.61
Germanate[13]	5.81	0.85	0.28

Fig.4 displays the measured 1.53 μm band fluorescence spectrum corresponding to Er^{3+}:^{4}I$_{13/2}$→^{4}I$_{15/2}$ transition of TZNS0 glass sample in the wavelength range of 1400-1700 nm. Because of the differences of the fluorescence spectra in different glass hosts, FWHM is often used as a semi-quantitative indication of the bandwidth. From the inset of Fig.4, it can be seen that the FWHM in the glass samples containing SiO$_2$ has a large value.
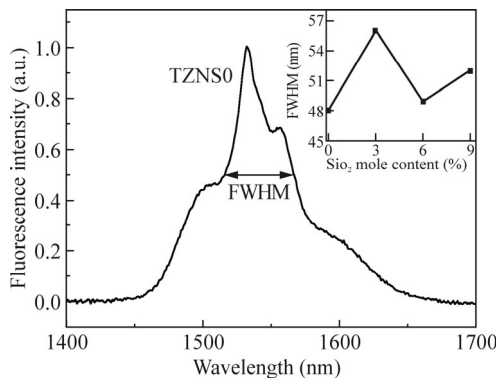
Fig.4 Fluorescence spectrum of TZNS0 glass sample (The inset is FWHM.)

Amplification characteristics of the EDFA gain medium are described mainly by the gain quality factor and bandwidth quality factor. The bandwidth quality factor is generally measured by the product of peak stimulated emission cross-section σ_e and FWHM[13,14]. The larger the product, the better the amplification bandwidth charteristics of the gain medium[15,16]. Tab.3 lists the relevant spectral parameters and bandwidth quality factors of Er^{3+} ions in the TZNS0-3 glasses. The FWHM is obtained directly from the measured fluorescence emission spectra, and the stimulated emission cross-section is obtained from the absorption cross-section σ_a of Er^{3+}:^{4}I$_{15/2}$→^{4}I$_{13/2}$ transition according to the McCumber theory[17]:

$$\sigma_e(\lambda)=\sigma_a(\lambda)\exp[(\varepsilon-h\nu)/kT] \ , \qquad (2)$$

where h is the Planck constant, k is the Boltzmann constant, ε is the net free energy required to excite one Er^{3+} from ^{4}I$_{15/2}$ to ^{4}I$_{13/2}$ level at temperature T and can be calculated using the method provided in Ref.[18].

Absorption cross-section σ_a is determined from the absorption spectra shown in Fig.3, which is related by:

$$\sigma_a(\lambda) = \frac{2.303}{NL}OD(\lambda) \ , \qquad (3)$$

where $OD(\lambda)$ is the optical density, N is the Er^{3+} ion doping concentration, and L is the thickness of glass sample. From Tab.3, it can be observed that the bandwidth quality factor in the glass samples containing SiO$_2$ has a larger value compared with that of glass sample without SiO$_2$. In addition, the bandwidth quality factor of glass samples developed in this paper is larger than that of silicate glass (22.0×10^{-20} cm^{2}nm)[19], germanate glass (23.9×10^{-20} cm^{2}nm)[20] and phosphate glass (23.7×10^{-20} cm^{2}nm)[21], which is attributed to the large stimulated emission cross- section and FWHM. Especially, the TZNS1 glass sample can be used as a potential host material for developing broadband EDFA in WDM system.
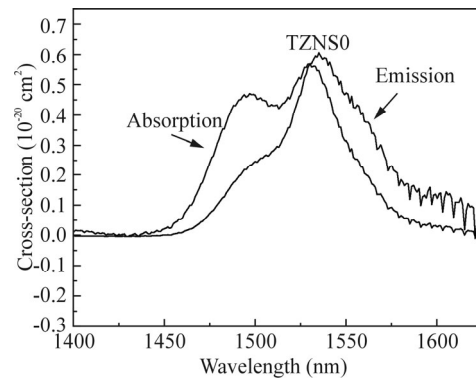
Fig.5 Stimulated absorption and emission cross-sections of TZNS0 glass sample

Tab.3 The stimulated absorption (σ_a) and emission (σ_e) cross-sections, FWHMs, and bandwidth quality factors of Er^{3+} in TZNS0—3 glass samples

Sample	σ_a (10^{-21} cm^2)	σ_e (10^{-21} cm^2)	FWHM (nm)	σ_e×FWHM (10^{-20} cm^{2}nm)
TZNS0	5.71	6.08	48	29.18
TZNS1	6.02	6.63	56	37.13
TZNS2	6.04	6.66	49	32.63
TZNS3	6.27	6.58	52	34.22

In this paper, the effects of SiO$_2$ on the spectroscopic properties and thermal stability of Er^{3+}-doped tellurite glasses are investigated. It is found that the introduction of an appropriate amount of SiO$_2$ can enhance the thermal stability of glass hosts. Meanwhile, the introduction of SiO$_2$ can also increase the FWHM and bandwidth quality factor of Er^{3+}. Therefore, as a glass host applied for the 1.53 μm broadband amplification, an appropriate amount of SiO$_2$ can be selectively introduced into the Er^{3+}-doped tellurite glasses.

References

[1]   R. El-Mallawany, A. Patra, C. S. Friend, R. Kapoor and P. N. Prasad, Opt. Mater. **26**, 267 (2004).

[2]   S. Wang, Y. X. Zhou, S. X. Dai, X. S. Wang, X. Shen, Y. Wu and X. C. Xu, Journal of Optoelectronics·Laser **22**, 12 (2011). (in Chinese)

[3]   T. Sasikala, M. L. Rama, K. Pavani and T. Chengaiah, J. Alloy Compd. **542**, 271 (2012).

[4]   Y. X. Zhou, X. C. Xu, F. Chen, J. H. Lin and G. B. Yang, Optoelectronics Letters **8**, 273 (2012).

[5]   T. F. Xu, X. D. Zhang, S. X. Dai, Q. H. Nie, X. Shen and X. H. Zhang, Physica B **389**, 242 (2007).

[6]   M. Okuno, B. Reynard, Y. Shimada, Y. Syono and C. Willaime, Phys. Chem. Minerals **26**, 304 (1999).

[7]   B. R. Judd, Phys. Rev. **127**, 750 (1962).

[8]   G. S. Ofelt, J. Chem. Phys. **37**, 511 (1962).

[9]   S. Tanabe, T. Ohyagi, N. Soga and T. Hanada, Phys. Rev. B **46**, 3305 (1992).

[10]   S. Tanabe, J. Non-Cryst. Solids **259**, 1 (1999).

[11]   M. J. Weber, Phys. Rev. **157**, 262 (1967).

[12]   J. Qiu, Y. Shimizugawa, Y. Iwabuchi and K. Hirao, Appl. Phys. Lett. **71**, 43 (1997).

[13]   S. C. Zheng, Y. W. Qi, S. X. Peng, D. D. Yin, Y. X. Zhou and S. X. Dai, Optoelectronics Letters **9**, 0461 (2013).

[14]   J. S. Wang, E. M. Vogel and E. Snitzer, Opt. Mater. **3**, 187 (1994).

[15]   M. Naftaly, S. Shen and A. Jha, Appl. Opt. **39**, 4979 (2000).

[16]   S. X. Dai, T. F. Xu, Q. H. Nie, X. Shen, J. J. Zhang and L. L. Hu, Acta Phys. Sin. **55**, 1479 (2006).

[17]   D. E. McCumber, Phys. Rev. **A299**, 134 (1964).

[18]   W. J. Miniscalco and R. S. Quimby, Opt. Lett. **16**, 258 (1991).

[19]   B. C. Hwang, S. Jiang, T. Luo, K. Seneschal, G. Sorbello, M. Morrell, F. Smektala, S. Honkanen, J. Lucas and N. Peyghambarian, IEEE Photon. Technol. Lett. **13**, 657 (2001).

[20]   H. Lin, E. Y. B. Pun, S. Q. Man and X. R. Liu, J. Opt. Soc. Am. B **18**, 602 (2001).

[21]   G. C. Righini, S. Pelli, M. Fossi, M. Brenci, A. A. Lipovskii, E. V. Kolobkova, A. Speghini and M. Bettinelli, Proc. SPIE **210**, 4282 (2001).